SMOLDERING COMBUSTION IN OIL SHALE: KINETICS PARAMETERS ESTIMATION USING INVERSE PROBLEMS

Marco A. B. Zanoni, mabzanoni@yahoo.com.br
Márcio F. Martins, marciofm@ct.ufes.br
Fabrício de S. P. Sisquini, fab_sisquini@hotmail.com
Federal University of Espírito Santo, LFTC, Vitória(ES), Brazil

Henrique M. da Fonseca, hmassard@mines-albi.fr
COPPE, Federal University of Rio de Janeiro, Rio de Janeiro, Brazil
Université de Toulouse, Mines Albi, CNRS, Centre RAPSODEE, Campus Jarlard, F-81013 Albi cedex 09, France

Abstract. Smoldering Combustion is a slow, low-temperature and flameless form of combustion and involves complex chemical reactions caused by the mechanisms of the solid fuel degradation. The smoldering combustion phenomena is found in smoking problems, deep seated fires, hidden fires, low oxygen combustion, in-situ combustion, fireflood and underground gasification. Thus, this paper proposes the estimation of the Arrhenius parameters for a reaction scheme of oil shale combustion in a fixed bed reactor. The kinetic parameters were estimated by using the Levenberg-Marquardt method through the ordinary least square norm minimization with the experimental data extracted from TGA experiments. A code was developed under a symbolic mathematics platform to solve the differential equations system and solve the inverse problem. The oil shale kinetics was established and its parameters were estimated in good agreement with the ones found in the literature.

Keywords: smoldering combustion, oil shale, parameter estimation, inverse problem, Levenberg-Marquardt method.

1. INTRODUCTION

Smoldering combustion (Palmer 1957), (Ohlemiller 1985) is a slow, low-temperature and flameless form of combustion and sustained by the heat evolved when oxygen directly attacks the surface of a condensed-phase fuel. This process is found in smoking problem, deep seated fires, hidden fires, low oxygen combustion, in-situ combustion, fireflood and underground gasification. The smoldering combustion phenomenon involves complex chemical reactions and is dominated by the kinetics of the oxidation of the solid. Thus, the kinetic parameters estimation is extremely important to build the reaction schemes. Because of the complex nature of the mechanism involving several simultaneous chemical reactions, a robust numerical procedure may be used.

Various methods to estimate kinetic parameters are available (Ozawa 1965), (Kissinger 1957), (Park et al. 1998). Some of them provide relatively net information about mass loss behavior, but calculation of kinetic parameters are based on the ordinary assumptions, and do not correspond to the complex chemical reactions during the thermal degradation (Kök et al. 2000). As example the graphical method (Kissinger 1957), (Ozawa 1965), and numerical fitting (Gal et al. 1972), (Horgan 1974) are limited only to one overall reaction. In the case of simultaneous reactions, a numerical procedure may be used, i.e., genetic algorithms (Rein et al. 2006) and inverse problem algorithms (Loulou et al. 2003), (Reverte et al. 2007).

Inverse problems can be found in many branches of science and engineering (Özisik et al. 2000), (Dantas et al. 2003), (Colombo 2007), (Mokhtari et al. 2010), typically when the observed data are used for the estimation of unknown quantities in the analysis of physical problems.. Here Thermogravimetric Analysis (TGA) is used as experimental data. TGA is an analytical technique used to determine changes in weight in relation to change in temperature. The difference in temperature between the sample and a reference material is recorded while both are subjected to the same heating programme. Thus, the present parameter estimation problem is solved with Levenberg-Marquardt's method (Levenberg 1944), (Marquardt 1963) by using TGA data to estimate the Arrhenius parameters of the reactions present in the pyrolysis process.

(Loulou et al. 2003) proposed the kinetics parameters estimation of cardboard pyrolysis by inverse problems using measurements collected from TGA. The kinetic model of cardboard decomposition, Eq. (1), proposed by (David et al. 2003) is present follow,

$$Cardboard \xrightarrow{k_1} Intermediate \xrightarrow{k_2} Char \tag{1}$$

where the cardboard is converted into an intermediate pseudo-species and the pseudo-species are converted into char.

(Reverte et al. 2007) describes additional numerical techniques to help to determine the kinetic parameters and to design a more robust parameter estimation tool using the kinetic model proposed by (Bradbury et al. 1979), presents in the Eq. (2) and Eq. (3) as follows,

$$Cellulose \xrightarrow{k_1} G_1 \tag{2}$$

$$Cellulose \xrightarrow{k_2} Char + G_2 \tag{3}$$

where, G_1 are the gaseous products and G_2 are the other gases.

(Sadhukhan et al. 2008) developed a simple mathematical model to describe the pyrolysis of a single biomass particle where a fully transient analysis involving a kinetic model coupled with heat transfer model has been presented. The Levenberg-Marquardt method was used for the kinetics parameters and heat of reaction estimation kinetics parameters and heat of reaction as presented in the Eq. (4) and Eq. (5).

$$Biomass \xrightarrow{k_1} (Volatiles + Gases) \tag{4}$$

$$Biomass \xrightarrow{k_2} Char \tag{5}$$

(Kowsary et al. 2009) used the Levenberg-Marquardt method for estimation of composite kinetics parameters during the cure process using a noise reduction technique based on wavelet transform to modify the sensor data before they are used by the IHCP (Inverse Heat Conduction Problem) methods.

For the present work oil shale was used as fuel particle to perform the oxidation process. Oil shales consist of a mineral porous matrix with the porosity filled with oil, called kerogen, representing 10–65% of the total mass. The mineral matrix consists of carbonates, quartz and clay (Saoiabi et al. 2001). Due to its complex composition when submitted to high temperatures many complex and parallel reactions takes place.

(Thakur et al. 1987) have shown that the thermal decomposition of oil shale involves two consecutive reactions with bitumen as an intermediate, as showed in Eq. (6-7). The kinetics parameters were estimated by using three different models, namely: Chen and Nuttall model, Coats and Redfern model, and Anthony and Howard model, while the isothermal TG data have been correlated by using the integral method.

$$Kerogen \xrightarrow{k_1} Bitumen + Gas \tag{6}$$

$$Bitumen \xrightarrow{k_2} Oil + Gas + Gas \tag{7}$$

(Barkia et al. 2003) analyzed the organic matter evolution and kinetics of combustion of Tarfaya and Timahdit oil shales by thermogravimetric analysis (TGA) and by differential thermal analysis (DTA). An agreement is observed between both techniques where it was found that combustion of organic matter occurs in two steps. Kissinger's method applied on experimental results gives activation energy of the same magnitude for the first step of both oil shales (103 kJ mol^{-1}) whereas the second is 148 kJ mol^{-1} for Timahdit and 118 kJ mol^{-1} for Tarfaya.

(Martins et al. 2010) proposed a realist reaction mechanism for the oil shale combustion. In this reaction mechanism, the oil shale dries when it is heated. The organic fraction then devolatilizes and produces volatile matter. Part of this volatile matter will condense to form liquid oil. A solid residue called fixed carbon is left in the mineral matrix. If the temperature is high, the carbonates in the oil shale are decarbonated, either partly or totally.

For all reactions mechanism, the Arrhenius equation, Eq. (8), indicates the rate of chemical reactions for each species,

$$k_i = A_i \exp\left(-\frac{E_i}{RT}\right) \quad with \quad (i = 1, 2, ..., 5) \tag{8}$$

where k is the Arrhenius constant, A is the pre-exponential factor, E is the activation energy, R is the ideal gas constant and T is the temperature. The subscript i indicates the number of chemical species.

To obtain a better understanding of the kinetics of oil shale combustion, the following goals were formulated to this work:

- To formulate a numerical procedure based on the inverse problem algorithm to estimate the Arrhenius parameters;
- To develop a code under the MATHEMATICA 7.0 platform to solve the differential equations system as well as the solution of the inverse problem of parameter estimation.

The numerical modeling of the Arrhenius equation requires the accurate knowledge of pre-exponential factor and the activation energy, both parameters that appear in the formulation. The identification of such parameters from the knowledge of mass loss measurements for each species is an *Inverse Problem*. Generally, inverse problems are

mathematically classified as *ill-posed,* in the sense that their solutions do not satisfy Hadamard's requirement of stability under small perturbations in the input data (Dantas et al. 2002). Despite the *ill-posed* character, the solution of an inverse problem can be obtained through its reformulation in terms of a *well-posed* problem, such as a minimization problem associated with some kind of regularization (stabilization) technique. Different methods based on such an approach have been successfully used in the past for the estimation of parameters and functions, in linear and non-linear inverse problems. They include the Levenberg-Marquardt method of parameter estimation (Dantas et al. 2002).

2. COMPOSITION AND THERMOCHEMICAL ANALYSIS OF OIL SHALE

The Thermogravimetric experiment adopted was used by (Martins et al. 2010) for oil shale combustion. The author used the oil shale layer of Timahdit in Morocco, where its overall composition is present in Tab. 1.

Table 1. Overall composition of the Timahdit oil shale.

Composition	Present Work (%)
Water	1.74
Organic Matter	15.42
Carbonates *(CaCO3)*	34.60
Inert Material	48.24

This oil shale is composed basically of inert material and carbonates, with 48.24 and 34.60 % wt., respectively. The amount of organic matter, 15.42 % wt. and water, 1.74 % wt., complement the overall composition of the oil shale.

2.1. ThermoGravimetric Analysis (TGA)

The TGA experiments were carried out using a TG – DSC 111 (Setaram) with the very sensitivity microbalance (limit of detection: 1μg). The temperature measurements were reproducible within ± 0.1 K at a temperature scale uncertainty ± 0.5 K. The samples with 40 mg approximately were heated at a heating rate of 10 K/min up to 800°C. Figure 1 shows the combustion of oil shale sample under air. TG experiments were repeated and show a good reproducibility, with a maximum deviation of a few %wt.
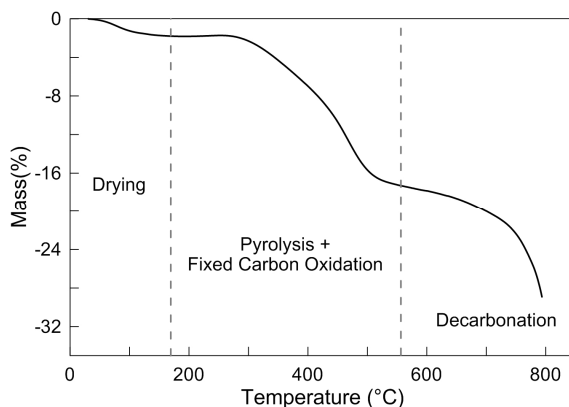

Figure 1.TGA of oil shale under air – heating rate a 10 k min^{-1}, (Martins et al. 2010).

The oil shale matrix is composed by a wide variety of minerals, fact that significantly complicates its thermal behavior. As a result, a diversity of reactions is brought about by the application of heat on the oil shale samples. In general, the following reactions can be identified:

(a) Evolution of water and gases;
(b) Conversion of kerogen to bitumen;
(c) Alteration of bitumen;
(d) Dissociation of bitumen from oils, gases and other compounds;
(e) Vaporization of oils;
(f) Burn-off of fixed carbon;

(g) Decomposition of organic residues and inorganic minerals.

In the decomposition of the oil shale sample, as shown in Fig.1, several stages are indicated:

(a) at temperatures between 50 and 150 °C, a mass loss of a few %wt. can be observed. It can be attributed to water evaporation;

(b) in the temperature range 150–550 °C an important mass loss can be observed. The differential scanning calorimetric test performed further, Fig. 2, shows two exothermic reactions, which occurs in the interval of 150- 550 °C. The first peak at 351 °C is due to the oxidation of the volatile matter (Kök et al. 1998) and the second at 461 °C is the oxidation of the carbonaceous residue (fixed carbon). In the oil shale combustion in a fixed bed only second peak occur, i.e., the fixed carbon oxidation, because the volatiles matters are released and does not oxidize.

(c) in the temperature range 550–800 °C, a last and important mass loss was observed. The differential scanning calorimetric presented in Fig. 2, indicates an endothermic reaction, attributed to the thermal decomposition of carbonates, producing carbon dioxide.
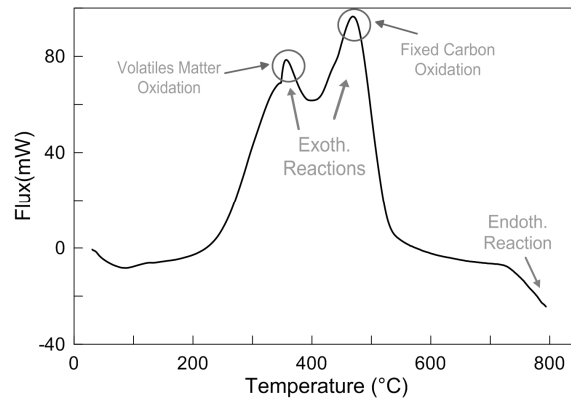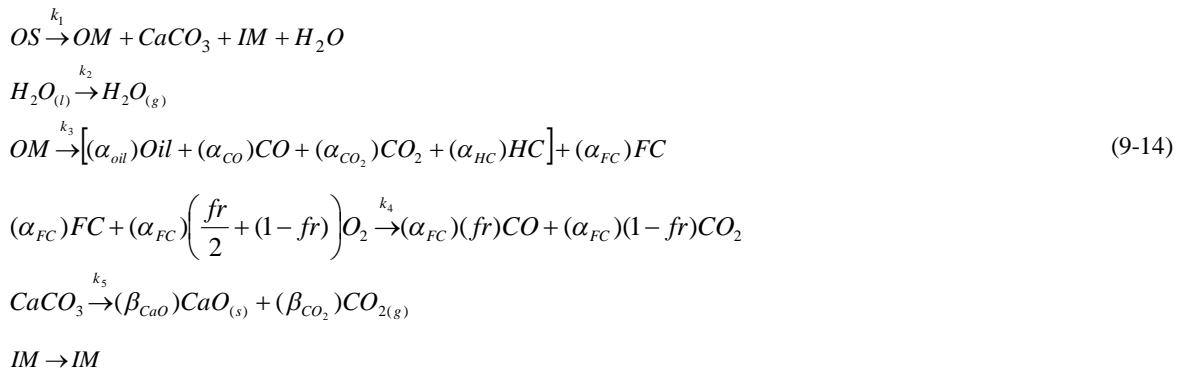
Figure 2. DSC of oil shale under air – heating rate a 10 k min^{-1}, (Martins et al. 2010).

There is a no clear separation between the two stages of organic matter decomposition and decarbonation along the test. For this reason, it was difficult to determine with accuracy the amount of organic matter and carbonates.

2.2. Kinetic Model

The oil shale combustion is extremely complex because of the presence of parallel and consecutive reactions. This paper proposes a more realistic reaction schemes for the oil shale combustion based on the experiments reported by (Martins et al. 2010), and presented in Eq. (9-14). The first reaction is the overall reaction of oil shale (OS) decomposition, resulting in Organic Matter (OM), Calcium Carbonates ($CaCO_3$), water (H_2O) and Inert Material (IM). The second reaction corresponds to the drying of oil shale where water undergoes evaporation at temperature range of 100-150 °C. The subsequent reaction involves the devolatilization of organic matter at temperature range of 150-550 °C, releasing Oil, CO, CO_2, hydrocarbons (HC) and fixed carbon (FC) in the solid matrix, where the fixed carbon is oxidized, releasing CO and CO_2. Finally, thermal decarbonation of $CaCO_3$ takes place in the temperature range 550 – 800 °C. In the solid residue after combustion remains an inert material.

$$OS \xrightarrow{k_1} OM + CaCO_3 + IM + H_2O$$

$$H_2O_{(l)} \xrightarrow{k_2} H_2O_{(g)}$$

$$OM \xrightarrow{k_3} \left[(\alpha_{oil})Oil + (\alpha_{CO})CO + (\alpha_{CO_2})CO_2 + (\alpha_{HC})HC \right] + (\alpha_{FC})FC \qquad (9\text{-}14)$$

$$(\alpha_{FC})FC + (\alpha_{FC})\left(\frac{fr}{2} + (1-fr) \right)O_2 \xrightarrow{k_4} (\alpha_{FC})(fr)CO + (\alpha_{FC})(1-fr)CO_2$$

$$CaCO_3 \xrightarrow{k_5} (\beta_{CaO})CaO_{(s)} + (\beta_{CO_2})CO_{2(g)}$$

$$IM \rightarrow IM$$

The stoichiometric coefficients, $\alpha_{Oil} = 0.53$, $\alpha_{CO} = 0.0102$, $\alpha_{CO2} = 0.0505$, $\alpha_{HC} = 0.1673$, $\alpha_{FC} = 0.242$, $\beta_{CaO} = 0.56$, $\beta_{CO2} = 0.44$ and $fr = 0.565$, were determined by (Martins et al. 2010). The rate reactions equations for the oil shale combustion, Eq. (15–25), may then be stated as follows:

$$\frac{dY_{H_2O}}{dt} = -k_2 (Y_{H_2O})^{n_2} \tag{15}$$

$$\frac{dY_{OM}}{dt} = -k_3 (Y_{OM})^{n_3} \tag{16}$$

$$\frac{dY_{Oil}}{dt} = (\alpha_{oil}) k_3 (Y_{OM})^{n_3} \tag{17}$$

$$\frac{dY_{HC}}{dt} = (\alpha_{HC}) k_3 (Y_{OM})^{n_3} \tag{18}$$

$$\frac{dY_{FC}}{dt} = (\alpha_{FC}) k_3 (Y_{OM})^{n_3} - (\alpha_{FC}) k_4 P_{O_2} (Y_{FC})^{n_4} (Y_{O_2})^{n_5} \tag{19}$$

$$\frac{dY_{O_2}}{dt} = -(\alpha_{FC}) \left(\frac{fr}{2} + (1 - fr) \right) k_4 P_{O_2} (Y_{FC})^{n_4} (Y_{O_2})^{n_5} \tag{20}$$

$$\frac{dY_{CO}}{dt} = (\alpha_{CO}) k_3 (Y_{OM})^{n_3} - (\alpha_{FC})(fr) k_4 P_{O_2} (Y_{FC})^{n_4} (Y_{O_2})^{n_5} \tag{21}$$

$$\frac{dY_{CO_2}}{dt} = (\alpha_{CO}) k_3 (Y_{OM})^{n_3} - (\alpha_{FC})(1 - fr) k_4 P_{O_2} (Y_{FC})^{n_4} (Y_{O_2})^{n_5} + (\beta_{CO_2}) k_5 (Y_{CaCO_3})^{n_6} \tag{22}$$

$$\frac{dY_{CaCO_3}}{dt} = -k_5 (Y_{CaCO_3})^{n_6} \tag{23}$$

$$\frac{dY_{CaO}}{dt} = (\beta_{CaO}) k_5 (Y_{CaCO_3})^{n_6} \tag{24}$$

$$Y = Y_{H_2O} + Y_{OM} + Y_{FC} + Y_{CaCO_3} + Y_{CaO} + Y_{IM} \tag{25}$$

where Y_i is the normalized mass of species i, n is its reaction order. The initial conditions for Eq. (15-25) were: $Y_{H_2O} = 0.01735$, $Y_{OM} = 0.1542$, $Y_{CaCO_3} = 0.346$, $Y_{IM} = 0.48245$, $Y_{O_2} = 0.02601$, $P_{O_2}=7.5\ kPa$ (Soni et al. 1979).

3. KINETICS PARAMETERS ESTIMATION

For the inverse problem of interest here, the parameters A_i and E_i, $i=2,…,5$ and n_j, $j=2,...,6$, are regarded as unknown quantities for each of Eq. (15-25). For the estimation of such parameters, we consider available the mass loss measurements Y_m. The subscript m refers to the time at which the measurements are taken, that is, t_m, for $m=1...N$. We note that the mass loss measurements may contain random errors, but all the other quantities appearing in the formulation of the direct problem are supposed to be known exactly.

Inverse problems are *ill-posed* (Dantas et al. 2002). Several methods of solution of inverse problems, such as the one used here, involve their reformulation in terms of *well-posed* minimization problems. By assuming additive, uncorrelated and normally distributed random errors, with constant standard deviation and zero mean, the solution of the present parameter estimation problem can be obtained through the minimization of the ordinary least-squares norm (Dantas et al. 2002). Such a norm, Eq. (26), can be written as

$$S(P) = [Y - M(P)]^T [Y - M(P)] \tag{26}$$

where $P=[A_i,E_i]$, for $i=2,...,5$, denotes the vector of unknown parameters. The superscript T above denotes transpose and *[Y-M(P)]* is given by Eq. (27)

$$[Y - M(P)]^T \equiv \left[\left(\vec{Y}_1 - \vec{M}_1 \right) \left(\vec{Y}_2 - \vec{M}_2 \right) ... \left(\vec{Y}_N - \vec{M}_N \right) \right] \tag{27}$$

where $\left(\vec{Y}_M - \vec{M}_M \right)$ is a row vector containing the differences between the measured and estimated mass loss at the measurement time *t*.

The present inverse problem of parameter estimation is solved with the Levenberg-Marquardt method of minimization of the least-squares norm. The Levenberg–Marquardt method is quite stable, powerful and straightforward (Özisik et al. 2000), and has been used to a diversity of inverse problems. Equation (28) shows the iterative procedure of the Levenberg-Marquardt method,

$$P^{(k+1)} = P^{(k)} + [(J^{(k)})^T J^{(k)} + \mu^{(k)} \Omega^{(k)}]^{-1} (J^{(k)})^T [Y - M(P^{(k)})] \tag{28}$$

where P denotes the vector of unknowns parameters, the subscript *(k)* denotes the iteration number, J is the sensitivity matrix, μ is a positive scalar named *damping parameter* and Ω, is a diagonal matrix . This iterative process contains oscillations and instabilities that difficult the convergence process. Thus, the purpose of the matrix term $\mu^k \Omega^k$ is to damp oscillations and instabilities due to the ill-conditioned character of the problem by making its components large as compared to those of $J^T J$, if necessary, and small when the iteration procedure advances to the solution of the parameter estimation problem. This automatic control makes the Levenberg-Marquardt method a quite robust and stable estimation procedure, so that an usual stopping criteria can be used (Dantas et al. 2002).

The sensitivity matrix, Eq. (29), is defined as

$$J = \left[\frac{\partial M^T(P)}{\partial P} \right]^T = \begin{bmatrix} \dfrac{\partial M_1}{\partial p_1} & ... & \dfrac{\partial M_1}{\partial p_m} \\ . & & . \\ . & & . \\ . & & . \\ \dfrac{\partial M_N}{\partial p_1} & ... & \dfrac{\partial M_N}{\partial p_m} \end{bmatrix} \tag{29}$$

The elements of the sensitivity matrix are the sensitivity coefficients. They are defined as the first derivative of the estimated mass with respect to each of the unknown parameters P_i, with $i = 2...5$.

The Levenberg-Marquardt algorithm used in this work was obtained from the built-in function *FindMinimum* of the *Mathematica* software. The stopping criterion used is when either the goals specified by *AccuracyGoal* or *PrecisionGoal* is achieved. *AccuracyGoal* is an option which specifies how many effective digits of accuracy should be sought in the final result and *PrecisionGoal* is an option which specifies how many effective digits of precision should be sought in the final result. In this work, both goals were set to 10^{-8}, the default value defined by *Mathematica*.

The standard deviation for the estimated parameters is given by:

$$\sigma_{P_i} = \sigma \sqrt{\left[J^T J \right]_{ii}^{-1}} \tag{30}$$

where σ is the standard deviations for TGA apparatus, with $\sigma = 10^{-4}$ kg, and J is the sensitivity matrix. Confidence intervals at the 99% confidence level for the estimated parameters are obtained by:

$$P_i - 2.576\sigma_{P_i} \le P_i \le P_i + 2.576\sigma_{P_i} \tag{31}$$

4. RESULTS AND DISCUSSION

4.1. Sensitivity Analysis

The sensitivity coefficient, J, is a measure of the sensitivity of the estimated mass loss M_i^k with respect to changes in the parameter P_i. A small value of sensitivity indicates that large changes in parameter P_i yield small changes in M_i^k (Özisik et al. 2000). Figure 3 shows the sensitivity analysis for the unknown parameters. The sensitivity coefficient with respect to the activation energy has a large magnitude for the pyrolysis/oxidation zone and decarbonation zone. This

indicates than the activation energy estimation can have a low estimation error. However, the estimation for the pre-exponential factor may have a large estimation error because the sensitivity coefficient with respect to these parameters has a low magnitude, as will be shown in the parameters estimation process.
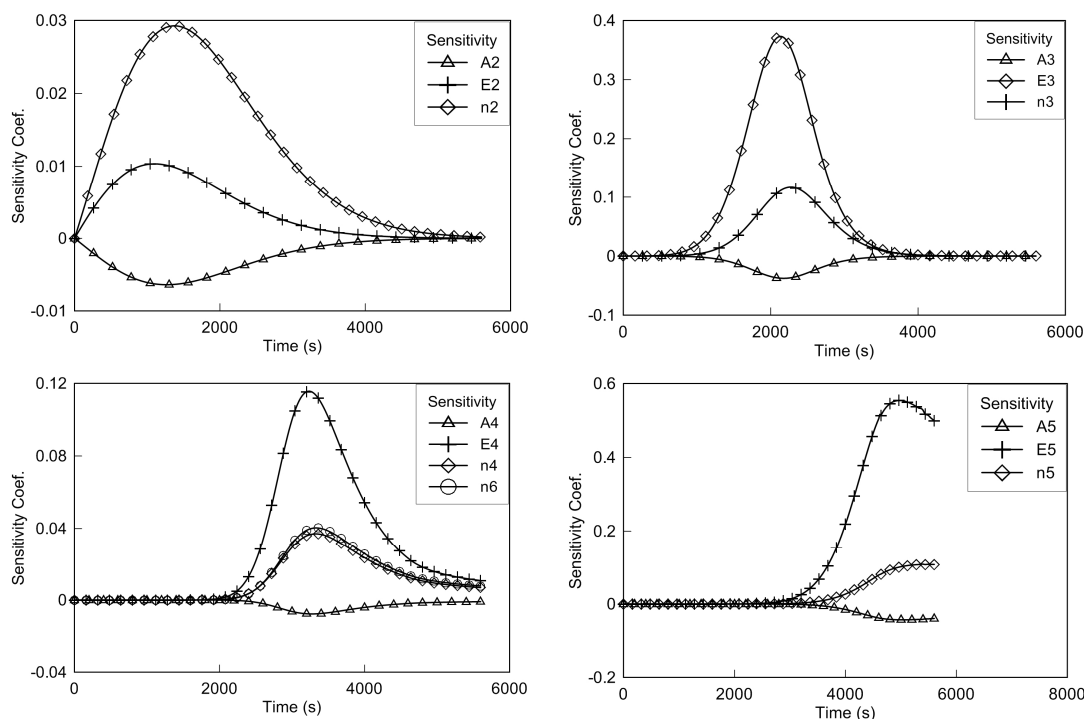

Figure 3. Sensitivity Analysis for the unknown parameters.

4.2. Parameter Estimation

Parameters A_i, E_i and n_i estimated with the Levenberg-Marquardt algorithm were obtained for a heat rate of 10K/min. The estimations of A_2, E_2 and n_2, A_3, E_3 and n_3, A_4, E_4, n_4 and n_6, A_5, E_5 and n_5 were made by using 40, 69 and 40 transient mass loss readings respectively. The initial guesses used in the iterative procedure of the Levenberg-Marquardt method were taken as 0.004 s^{-1} for A_2, 55000 Jxmol^{-1} for E_2 and 1.0 for n_2, 40.0 s^{-1} for A_3, 50000 Jxmol^{-1} for E_3 and 1.3 for n_3, 550.0 s^{-1} for A_4, 52400 Jxmol^{-1} for E_4, 1.3 for n_4 and 1.3 for n_6, and 500.0 s^{-1} for A_5, 110000 Jxmol^{-1} for E_5 and 1.4 for n_5. These adopted values were chosen by comparing with values found to the similar reactions available in the literature.

The oil shale sample, in drying zone, lost a small amount of water. This reaction occurs in a time range of 0-721 s and the Arrhenius parameters estimated were $E_2=55435.6$ Jxmol^{-1}, $A_2=5.3x10^7$ s^{-1} and $n_2=1.932$. In the time range of 722-3100 s, the activation energy and pre-exponential factor found for pyrolysis and oxidation zone were $E_3=50136.3$ Jxmol^{-1}, $A_3=29.766$ s^{-1}, $n_3=1.263$, $E_4=100345$ Jxmol^{-1}, $A_4=9.715x10^6$ s^{-1}, $n_4=1.279$ and $n_6=1.285$ and the interval between 3100-4618 s, the Arrhenius parameters found were $E_5=158788$ Jxmol^{-1}, $A_5=475605$ s^{-1} and $n_5=1.594$ for the decarbonation zone. Table 2 presents the Arrhenius parameters estimation and the error for this estimation.

The errors of estimation for the pre-exponential factor, A_2, activation energy, E_2, and reaction order, n_2, in the drying zone were 35.67%, 1.272% and 1.296%, respectively. In the pyrolysis/oxidation zone the errors were 3.163% for A_3, 0.166% for E_3, 0.615% for n_3, 36.738% for A_4, 1.694% for E_4, 4.088% for n_4 and 4.494% for n_6. In the decarbonation zone, the errors were 0.846% for A_5, 0.04% for E_5 and 0.028% for n_5. These large errors for parameters A_2 and A_4 are attributed to difficulty in separating the areas in which the reactions occur because there is no clear separation between the two stages of water and fixed carbon oxidation along the test. The activation energy estimation is better than pre-exponential factor estimation presenting a small magnitude for the estimation error, as evidenced by sensitivity analysis.

Table 3 presents the parameters estimated in this work compared with results found in literature. One can see that despite a discrepancy between the values found for several authors, the results obtained herein are in good agreement with the literature.

Table 2. Results for parameters estimation for oil shale combustion.

Parameters	Estimated	Error (%)
A_2 (s^{-1})	5.300×10^7	35.674
E_2 (Jxmol^{-1})	55.435×10^3	1.272
n_2 (-)	1.932	1.296
A_3 (s^{-1})	2.976×10^1	3.163
E_3 (Jxmol^{-1})	50.136×10^3	0.166
n_3 (-)	1.263	0.615
A_4 (s^{-1})	9.715×10^6	36.738
E_4 (Jxmol^{-1})	100.345×10^3	1.694
n_4 (-)	1.279	4.088
n_6 (-)	1.285	4.494
A_5 (s^{-1})	475.605×10^3	0.846
E_5 (Jxmol^{-1})	158.788×10^3	0.041
n_5 (-)	1.594	0.028

Table 3. Activation energy and pre-exponential factor for oil shale combustion.

	Drying Zone			Pyrolysis/Oxidation Zone							Decarbonation Zone		
Literature	E_2 (J mol^{-1})	A_2 (s^{-1})	n_2 (-)	E_3 (J mol^{-1})	A_3 (s^{-1})	n_3 (-)	E_4 (J mol^{-1})	A_4 (s^{-1})	n_4 (-)	n_6 (-)	E_5 (J mol^{-1})	A_5 (s^{-1})	n_5 (-)
Present Work	55.4×10^3	5.3×10^7	1.93	50.1×10^3	2.97×10^1	1.26	100.3×10^3	9.71×10^7	1.27	1.28	158.788×10^3	475.6×10^3	1.59
(Sonibare et al. 2005)	—	—	—	75.0×10^3	3.95×10^{-1}	—	—	—	—	—	—	—	—
(Kök et al. 2004)	—	—	—	36.1×10^3	—	—	58.7×10^3	—	—	—	—	—	—
(Kök et al. 1999)	—	—	—	46.0×10^3	8.1×10^{-3}	—	—	—	—	—	—	—	—
(Galwey et al. 1997)	—	—	—	—	—	—	—	—	—	—	205.0×10^3	—	—
(Liu et al. 2003)	—	—	—	—	—	—	—	—	—	—	215.0×10^3	—	—
(Martins et al. 2010)	—	—	—	—	—	—	—	—	—	—	135.0×10^3	4.46×10^2	—
(Barkia et al. 2003)	—	—	—	103.0×10^3	—	—	148.0×10^3	—	—	—	—	—	—

The comparison between the numerical solution and experimental data is showed in Fig. 4. The numerical solution is in good agreement with the experimental data with a maximum deviation of a few%.
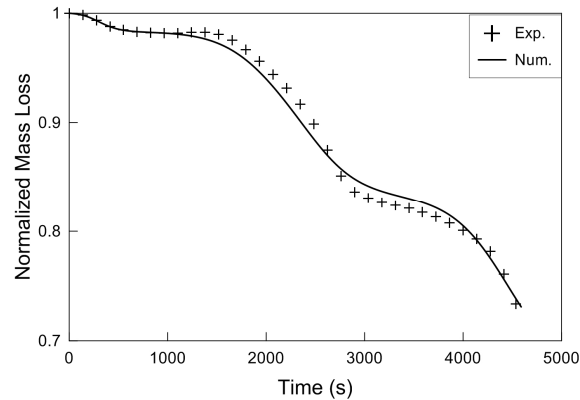

Figure 4. Comparison between numerical solution and experimental data.

5. CONCLUSION

A numerical routine to estimate the kinetics of thermochemical degradation for solid fuels was developed with successes. This routine applies both inverse problem and TGA experiments to propose a new reaction mechanism. Here, oil shale kinetics was established and its parameters estimated with accuracy, with a low error for the activation energy and a large error for the pre-exponential factor in drying zone and pyrolysis and oxidation zone. These large errors are attributed to difficulty in separating the areas in which the reactions occur because there is no clear separation between the two stages of water and fixed carbon oxidation along the test.

By exploiting the TG data, it was established that the oil shale sample contains 1.74% of moisture and produced 8.0% of Oil, 2.5% of HC and 1.9% of FC when heated from 150 to 600ºC. The oil shale also contains 48.68% of inert materials and 34.60% carbonates which produced 16.9 % of CO_2, 2.2% of CO and 20% of CaO. Some of these values were used as initial conditions in the system equations and showed be good in the system solution approach.

The estimated parameters A_i and E_i are in good agreement with the ones found in the literature.

6. ACKNOWLEDGEMENTS

7. REFERENCES

Barkia, H., L. Belkbir, et al. (2003). "Oxidation kinetics of timahdit and tarfaya moroccan oil shales." Journal of Thermal Analysis and Calorimetry 71(1): 97-106.

Bradbury, A. G. W., Y. Sakai, et al. (1979). "A kinetic model for pyrolysis of cellulose." Journal of Applied Polymer Science 23(11): 3271-3280.

Colombo, F. (2007). "An inverse problem for a parabolic integrodifferential model in the theory of combustion." Physica D: Nonlinear Phenomena 236(2): 81-89.

Dantas, L. B., H. R. B. Orlande, et al. (2002). "Estimation of dimensionless parameters of Luikov's system for heat and mass transfer in capillary porous media." International Journal of Thermal Sciences 41(3): 217-227.

Dantas, L. B., H. R. B. Orlande, et al. (2003). "An inverse problem of parameter estimation for heat and mass transfer in capillary porous media." International Journal of Heat and Mass Transfer 46(9): 1587-1598.

David, C., S. Salvador, et al. (2003). "Determination of a reaction scheme for cardboard thermal degradation using thermal gravimetric analysis." Journal of Analytical and Applied Pyrolysis 67(2): 307-323.

Gal, A., J. M. Soper, et al. (1972). "A shell-model analysis of [Lambda] binding energies for the p-shell hypernuclei II. Numerical Fitting, Interpretation, and Hypernuclear Predictions." Annals of Physics 72(2): 445-488.

Galwey, A. K. and M. E. Brown (1997). "Arrhenius parameters and compensation behaviour in solid-state decompositions." Thermochimica Acta 300(1-2): 107-115.

Horgan, R. (1974). "Baryon spectroscopy and the quark shell model (II). Numerical fitting to the data and the baryonic predictions." Nuclear Physics B 71(3): 514-545.

Kissinger, H. E. (1957). "Reaction kinetics in differential thermal analysis." Analytical chemistry v. 29(n. 11): p. 1702-1706.

Kök, M. and M. Pamir (1998). "ASTM Kinetics of Oil Shales." Journal of Thermal Analysis and Calorimetry 53(2): 567-575.

Kök, M., G. Pokol, et al. (2004). "Combustion characteristics of lignite and oil shale samples by thermal analysis techniques." Journal of Thermal Analysis and Calorimetry 76(1): 247-254.

Kök, M., J. Sztatisz, et al. (1999). "Characterization of Oil Shales by High Pressure DSC." Journal of Thermal Analysis and Calorimetry 56(2): 939-946.

Kök, M. V. and M. R. Pamir (2000). "Comparative pyrolysis and combustion kinetics of oil shales." Journal of Analytical and Applied Pyrolysis 55(2): 185-194.

Kowsary, F., M. Sefidgar, et al. (2009). "Estimation of kinetic parameters of composite materials during the cure process using the combined wavelet regularization method." Journal of Engineering Physics and Thermophysics 82(5): 949-955.

Levenberg, K. (1944). "A method for the solution of certain non-linear problems in least square." Q Appl Math 2(2): 164–168.

Liu, J. and J. Zhang (2003). "Assessment of the apparent activation energies for gas/solid reactionscarbonate decomposition." JOURNAL OF UNIVERSITY OF SCIENCE AND TECHNOLOGY BEIJING Vol. 10 P.25-29.

Loulou, T., S. Salvador, et al. (2003). "Determination of Reaction Parameters for Cardboard Thermal Degradation Using Experimental Data." Chemical Engineering Research and Design 81(9): 1265-1270.

Marquardt, D. W. (1963). "An algorithm for least square estimation of nonlinear parameters." J Soc Ind Appl Math 11(2): 431–441.

Martins, M. F., S. Salvador, et al. (2010). "Co-current combustion of oil shale - Part 1: Characterization of the solid and gaseous products." Fuel 89(1): 144-151.

Martins, M. F., S. Salvador, et al. (2010). "Co-current combustion of oil shale - Part 2: Structure of the combustion front." Fuel 89(1): 133-143.

Mokhtari, S., A. Vatani, et al. (2010). "Comparative study of kinetic modeling for the oxidative coupling of methane by genetic and marquardt algorithms." Journal of Natural Gas Chemistry 19(3): 293-299.

Ohlemiller, T. J. (1985). "Modeling of smoldering combustion propagation." Progress in Energy and Combustion Science 11(4): 277-310.

Ozawa, T. (1965). "A new method of analyzing thermogravimetric data." Bulletin Of The Chemical Society of Japan v. 38(n.11): p. 1881-1886.

Özisik, M. N. and H. R. B. Orlande (2000). "Inverse heat transfer." 35 - 114.

Palmer, K. N. (1957). "Smouldering combustion in dusts and fibrous materials." Combustion and Flame 1(2): 129-154.

Park, T.-Y. and G. F. Froment (1998). "A hybrid genetic algorithm for the estimation of parameters in detailed kinetic models." Computers & Chemical Engineering 22(Supplement 1): S103-S110.

Rein, G., C. Lautenberger, et al. (2006). "Application of genetic algorithms and thermogravimetry to determine the kinetics of polyurethane foam in smoldering combustion." Combustion and Flame 146(1-2): 95-108.

Reverte, C., J.-L. Dirion, et al. (2007). "Kinetic model identification and parameters estimation from TGA experiments." Journal of Analytical and Applied Pyrolysis 79(1-2): 297-305.

Sadhukhan, A. K., P. Gupta, et al. (2008). "Modelling and experimental studies on pyrolysis of biomass particles." Journal of Analytical and Applied Pyrolysis 81(2): 183-192.

Saoiabi, A., A. Doukkali, et al. (2001). "Schistes bitumineux de Timahdit (Maroc) : composition et propriétés physicochimiquesTimahdit (Morocco) oil shales: composition and physicochemical properties." Comptes Rendus de l'Académie des Sciences - Series IIC - Chemistry 4(5): 351-360.

Soni, Y. and W. J. Thomson (1979). "Oxidation Kinetics of Oil Shale Char." Industrial & Engineering Chemistry Process Design and Development 18(4): 661-667.null

Sonibare, O. O., O. A. Ehinola, et al. (2005). "Thermal and geochemical characterization of Lokpanta oil shales, Nigeria." Energy Conversion and Management 46(15-16): 2335-2344.

Thakur, D. S. and H. E. Nuttall (1987). "Kinetics of pyrolysis of Moroccan oil shale by thermogravimetry." Industrial & Engineering Chemistry Research 26(7): 1351-1356.null

8. RESPONSIBILITY NOTICE

The authors are the only responsible for the printed material included in this paper.